Journal of Computers Vol. 31 No. 3, 2020, pp. 289-302
doi:10.3966/199115992020063103023

Navigation Stability Analysis of Amphibious Armored Vehicles by Computer Virtual Reality Technology

Jian-Hua Luo[1], Chao Song[2*], Ling Li[3]

[1] Military Exercise and Training Center, Armored Forces Academy, Beijing, China
jh.luo@vip.sina.com

[2] Department of Weapons and Control, Armored Forces Academy, Beijing, China
andysong2010@qq.com

[3] Beijing Satellite Navigation Center, Beijing, China
13601114890@163.com

Received 15 March 2020; Revised 1 April 2020; Accepted 15 April 2020

Abstract. To analyze and study the navigation performance of amphibious armored vehicles and improve the in-water performance of amphibious armored vehicles, thereby realizing the development of amphibious vehicles in the context of computer virtual technology, this study starts from the discussion of driving simulators and explores the navigation stability of the amphibious armored vehicle. First, the slope resistance, air resistance, soil adhesion, and other factors are considered, and the dynamic models of the amphibious armored vehicle traveling on the ground and the water from the land are established. The latter is simulated and analyzed. Second, the model test and integration are combined with the system identification thought of the genetic algorithm, and a discriminant model for the rolling motion of the amphibious armored vehicle is constructed. Finally, the application effect of the discriminative model is verified by the experimental design and lateral body arrangement of the vehicle on the water. The results show that the acceleration, speed, and position changes of the vehicle are consistent with the actual situation, and the simulation analysis works well. The relative error rate of the predicted value curve obtained by the identification method proposed in this study is smaller than the calculated value of the linear equation and is closer to the experimental measurement value. The method and the corresponding mathematical equation model are reliable and applicable. There are differences in the vehicle rolling amplitude changes under different side body schemes. Schemes 1 and 2 show larger rolling amplitude changes. The results of segment identification indicate that the scheme in this study can explain the waveform phenomenon to a certain extent. The exploration of the rolling motion of the amphibious armored vehicle based on wave resistance on the water is of great significance in the research of its navigation stability on the water.

Keywords: amphibious armored vehicle, driving simulator, dynamics model, rolling motion, system identification

1 Introduction

The research on amphibious vehicles in China started in the 1960s. Among them, amphibious armored vehicles can travel on land and water. Overcoming water obstacles and ensuring the passability of water and land junctions are its main uses. However, the speed of water travel is difficult to meet the requirements of use, which is very critical for improving the water use characteristics of amphibious armored vehicles [1]. Due to the slow development, the technical level of amphibious vehicles in China lags behind compared with other countries. Thus, the improvement of its water use performance is

* Corresponding Author

critical. For the improvement of water speed and stability, internal parameters including engine power and water-resistance are the major influencing factors [2]. Previous works have improved the water speed of amphibious vehicles. At the same time, studies on amphibious armored vehicles are various; however, most of them focus on land performance, while studies on learning and navigation stability in water are rare.

This study takes amphibious armored vehicles as the research object, combines driving simulator with the construction of the vehicle hydrodynamic model. Considering factors such as slope resistance and air resistance, the dynamic model of amphibious armored vehicles traveling on land and entering the water from land is constructed. Based on the combination of model tests and system identification ideas, the wave resistance rolling motion mathematical identification model is constructed, and the identification effect of the model is verified through the experimental design and the layout of the side body plan. This study aims to provide some reference for the research on the navigation stability of amphibious armored vehicles in the water.

2 Literature Review

The T-40 surface tank developed by the Soviet Union in 1940 was driven by the propeller at the rear at a speed of 5-6 km/h. In the 1960s, it successfully installed a BTP-60 wheeled transport vehicle that made it capable of floating on water. The ВМП-3 surface tank developed by Russia in 1987 could reach a speed of 10 km/h on water and could turn in the water. The AAAV high-speed advanced amphibious assault vehicle successfully developed by the United States in the 1980s had a common speed of 37 km/h on the sea and a maximum speed of 46 km/h. The FV432 tracked floating armored vehicle developed by the UK in 1971 had a maximum water speed of 6.6 km/h, and the high-speed wheeled amphibious vehicle Aquada could reach a speed of 50 km/h on the water. The highest water speed of Splash developed by Switzerland could reach 80 km/h [3-4]. In China, the speed of the 63-type A surface tank can reach 18.61 km/h. The highest speed of the first amphibious car in China reached 12 km/h. The maximum speed of XBH8×8-2 of a certain vehicle company in Yiwu City, Zhejiang Province is 12 km/h on the water. The two degree-of-freedom (DOF) tracked vehicle mathematical model is the earliest proposed tracked vehicle dynamics model [5]. Later, some scholars proposed a three-dimensional tracked vehicle model [6] and a composite tracked model [7] for analyzing the dynamic performance of tracked vehicles. By using MATLAB/Simulink, the transmission system model of the tank is built [8-9]. Based on the numerical model of the underwater vibration of the amphibious vehicle, the motion of the amphibious tank on the water is calculated based on the numerical integration method, and the principles for the amphibious vehicle to enter and exit water are discussed in detail. There have been many studies on the performance of amphibious armored vehicles. However, studies on land performances are more, while the studies on vehicle dynamics and navigation stability in water are rarely reported.

3 Method

3.1 Driving Simulator Based on Virtual Reality Technology

Virtual reality (VR) technology is a new technology developed in the 20th century. This technology includes computer information technology and simulation technology. It is realized by the simulation of the virtual environment by computers. At present, VR technology has developed into a new field of science and technology, which has been applied in all walks of life [10-11]; also, the VR technology is applicable to driving simulators based on amphibious armored vehicles. The driving simulator is a simulation device. It uses computer VR technology to realistically simulate the driving behavior of vehicles, including amphibious armored vehicles. Therefore, the simulation device is widely used in driving training. The earliest development of driving simulators is for the smooth development of simulation training, which can be specifically divided into tank driving simulators, flight training simulators, and car driving simulators [12-13]. The entire system of the driving simulator is composed of the driver, physical effect equipment, and model solving system. The driver is in a sensory environment formed by physical effect device simulation. The physical effect device includes a simulated cockpit, a sound effect system, a motion system, and a visual system; meanwhile, the model calculating component

provides corresponding simulation data to simulate the physical environment to the physical effect device. In the driving simulator, the real-time computer simulation system, motion system, sound effect system, simulated cockpit, and command console are the key subsystems. The real-time computer simulation system is the core of this. The simulation system is mainly composed of real-time simulation computer software and simulation software. The role of the software component is to set the information and complete the transmission of data information to each subsystem, thereby outputting the posture and position of the armored vehicle and finally completing the simulation of the driving environment.

Before the training of the driving simulator begins, various software programs need to be processed to make it run normally/ Then, the commander completes the setting of the initial conditions so that the driver can perform various training tasks. The implementation process of the entire driving simulator system includes three major components: system startup and initialization, training work development, and system exit. The first and third components mentioned above are unique in the driving simulator. The operating flowchart of the corresponding driving simulator is shown in Fig. 1 below.

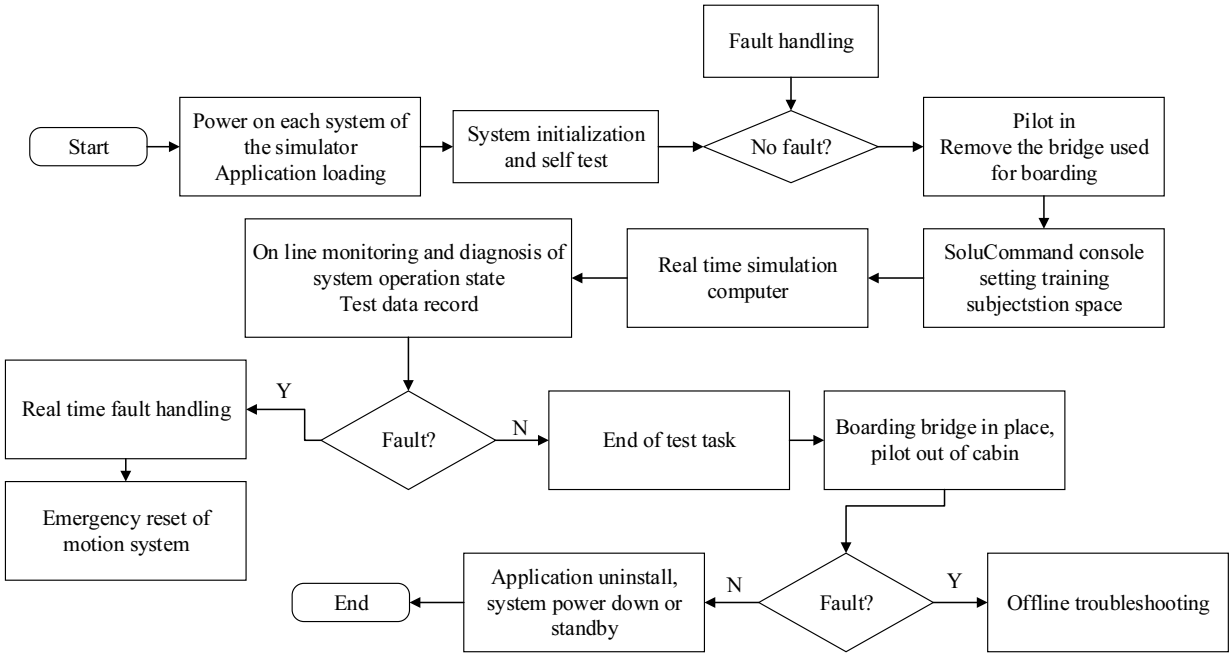

Fig. 1. Operation realization process of the driving simulator

3.2 Dynamic Model Construction of Amphibious Armored Vehicles

The vehicle dynamic model is one of the key components of the real-time computer simulation subsystem in the driving simulator [14]; thus, the vehicle dynamic model has a direct effect on the working effect of the driving simulator. To analyze the hydrodynamics of amphibious armored vehicles, a dynamic model of amphibious armored vehicles traveling on land and entering the water from land is constructed.

3.2.1 The Dynamic Model of Land Travel of the Amphibious Armored Vehicle

In the construction of an on-road driving dynamics model of an amphibious armored vehicle, the entire vehicle is considered as a single rigid body, and the impact of external environments such as slope resistance, air resistance, and soil adhesion is considered. If the amphibious armored vehicle is traveling on a vertical slope that is angled to the ground without tilting, the motion equation of the mass center of the amphibious armored vehicle can be described by Equation (1) below. Considering the additional kinetic energy caused by the internal component rotation of the armored vehicle that makes the armored vehicle appear to have an increase in mass, the description of the additional coefficient of the mass of the amphibious armored vehicle is shown in Equation (2) below. When the torque transmitted from the engine to the driving wheels acts on the ground via the track, the ground has traction on the vehicle in the opposite direction of the armored vehicle. As the traction increases, the corresponding compression

deformation of the soil also increases. At the same time, the rearward displacement of the contact portion of the track with the ground also increases. The adhesion force of the vehicle during driving on the ground is different. If the traction force received by the vehicle is greater than the maximum adhesion force given to the ground, it will cause the vehicle to slip. In general, the maximum adhesion force that the ground can withstand is defined as the result of multiplying the adhesion coefficient by the normal load given to the ground by the vehicle body, and its corresponding equation is expressed as shown in Equation (3) below. When an armored vehicle runs on a plastic road, it will cause the road to sink. The head resistance is the maximum single driving resistance of the vehicle generated by the front of the track on the road. At this time, the head resistance is generated by the internal friction, and the corresponding calculation of the ground resistance is shown in Equation (4) below. During the driving of amphibious armored vehicles, the amount of road subsidence is related to the pressure on the road surface and the nature of the soil. This study uses the Bekker Equation to characterize the relationship between soil subsidence and pressure, as shown in Equation (5) below. When the vehicle is driving at a high speed or the wind speed is large, the influence of air resistance should be considered, and the corresponding equation is expressed as shown in the following Equation (6).

$$F_T - F_G \cdot \sin\alpha - F_{BUG} - F_L = \delta \cdot \frac{F_G}{g} \cdot \frac{dv}{dt} \tag{1}$$

Where: F_T is the vehicle traction, F_G is the vehicle gravity, F_{BUG} is the head resistance, F_L is the air resistance, α is the sine angle of gravity, δ is the vehicle mass additional coefficient, g is the acceleration of gravity, v is the speed of the vehicle, and t is time.

$$\delta = 1.0 + \frac{G_L}{G} + \frac{g}{Gr_z^2}\sum I_i i_i^2 \tag{2}$$

Where: G_L is the weight of the track, G is the weight of the vehicle, I_i is the moment of inertia of the i-th relative rotating component, i_i is the transmission ratio of the i-th relative rotating component to the driving wheel, and r_z is the radius of the driving wheel.

$$F_{T\max} = u_R F_N \tag{3}$$

Where: u_R is the corresponding adhesion coefficient of the ground, and F_N is the ground supporting force.

$$F_{BUG} = 2 \times b_k \times t_g \times P_0^{'} \times \left(\tan\rho + \tan\beta\right) \tag{4}$$

Where: b_k is the track width, t_g is the deformation height of the pavement, $P_0^{'}$ is the effective ground pressure, ρ is the ground friction angle, and β is the track entry angle.

$$P = \left(\frac{k_c}{b_k} + k_\phi\right) t_g^n \tag{5}$$

Where: k_c is the cohesion modulus of the soil, b_k corresponds to the width of the track, k_ϕ corresponds to the internal friction modulus of the soil, and n is the soil deformation index.

$$F_L = \frac{\rho_L}{2} \cdot V_{rel}^2 \cdot C_w \cdot A \tag{6}$$

Where: ρ_L is the air density, V_{rel} is the relative speed between the air and the vehicle, C_w is the resistance coefficient of the air, and A is the projected area facing the wind.

3.2.2 The Dynamic Model of the Amphibious Armored Vehicle Entering the Water from the Land

The entry of water of amphibious vehicles refers to the process by which the vehicle uses its land travel capability to enter the water surface via land or landing ships [15]. The water entering angle refers

to the maximum slope angle that can be overcome during the smooth water entering process through the bank slope under the condition of the total mass of the battle. In most cases, when the amphibious armored vehicles enter the water, at first, there will be buoyancy due to flooding. Therefore, the normal pressure of the vehicle on the slope and the magnitude of buoyancy show a negative correlation. The forward process of the vehicle is accompanied by the traction force continues to decrease, while the resistance continues to increase until the resistance increases to equal to the traction force. If the vehicle floats up, it indicates that the vehicle has successfully entered the water. To characterize the dynamics of the vehicle and its instantaneous position in space, the body coordinate system o-xyz and inertial coordinate system O-XYZ shown in Fig. 2 below are established, where the body coordinate system is fixed to the vehicle body, the origin o corresponds to the gravity center of the vehicle G, the horizontal axis corresponds to the front of the vehicle, and the z-axis corresponds to the vehicle directly below. Besides, the inertial coordinate system is fixed to the ground, which corresponds to the body coordinate system of the vehicle at the initial position. Considering that the representation of the vehicle speed and position change is more representative in front of and directly below the vehicle, the x (X) direction and z (Z) direction are selected as the premise of the data representation for the following exploration.

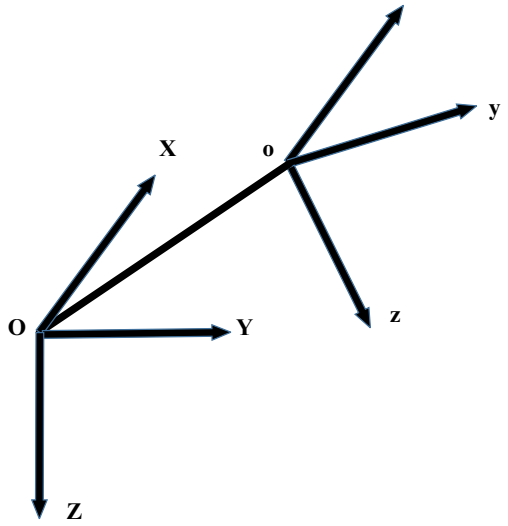

Fig. 2. Establishment of the coordinate system

According to the difference between the buoyant moment and gravity moment, the water entering of the armored vehicle can be divided into two stages. In the first stage, the buoyancy moment is always smaller than the gravity moment. At this time, the overall load of the vehicle is above the ramp and no rotation has occurred. Therefore, the speed of the vehicle entering the water is slow, and the water-resistance can be ignored. From the perspective of buoyancy, according to Archimedes' principle, buoyancy is always equal to the weight of the volume of water discharged by the vehicle. As the vehicle moves forward, the drainage volume increases continuously; thus, the buoyancy continues to increase. From the perspective of the ground support force, the normal support force acting on the track shows a trapezoidal distribution. With the increase of buoyancy, the ground support force shows a decreasing change. Similar to the continuous change of the position of the buoyancy center, the position of the supporting point of action is also constantly changing. The traction force received by the vehicle is related to the torque transmitted by the engine to the driving wheels. As the road surface of the vehicle changes from dry soil to wet soil, the corresponding adhesion coefficient becomes smaller. On this basis, the construction of the hydrodynamic model of the amphibious armored vehicle at this stage is shown in Equation (7) below.

$$\begin{bmatrix} \sum F_{\mathrm{x}} = F_T - F_{BUG} + (F_G - Q)\sin\alpha - F_{WAV}\sin\beta = \delta\dfrac{F_G}{g}\dfrac{dv_x}{dt} \\ \sum F_y = 0 \\ \sum F_z = (F_G - Q)\cos\alpha - F_{WAV}\cos\beta - F_N = \delta\dfrac{F_G}{g}\dfrac{dv_z}{dt} \end{bmatrix} \tag{7}$$

Where: Q represents buoyancy, F_{WAV} is wave force, and β is the angle between the front skis and the coordinate plane.

In the second stage, the moment corresponding to buoyancy starts to be greater than the moment corresponding to gravity, and the vehicle starts to rotate. At this time, the direction of the ground support force is perpendicular to the ground. Due to the buoyant moment, the front section of the track of the armored vehicle is no longer in contact with the ground, and only a part of the track in the adjacent position is in contact with the ground and bears the weight of the armored vehicle, which causes the traction to become a part of the traction in stage 1. On this basis, the construction of the hydrodynamic model of the amphibious armored vehicle in the second stage is shown in Equation (8) below.

$$\begin{bmatrix} \sum F_{\mathrm{x}} = (F_T - F_{BUG})\cos\theta + F_N\sin\theta + (F_G - Q)\sin(\alpha - \theta) - F_{WAV}\sin\beta = \delta\dfrac{F_G}{g}\dfrac{dv_x}{dt} \\ \sum F_y = 0 \\ \sum F_z = (F_G - Q)\cos(\alpha - \theta) - F_N\cos\theta + (F_T - F_{BUG})\sin\theta - F_{WAV}\cos\beta = \delta\dfrac{F_G}{g}\dfrac{dv_z}{dt} \end{bmatrix} \tag{8}$$

Where: θ is the rotation angle of the vehicle around the y axis.

3.3 System Identification of Vehicle Rolling Motion

The research on the stability of navigation on the water mainly involves two aspects; one is the wave resistance of surface navigation, and the other is the attitude stability [16-17]. Since the rolling motion is a key part of the wave resistance research, this study is performed based on it. Theoretical analysis method, numerical analysis method, and model test method are commonly used methods to study the rolling motion. The theoretical analysis method is effective and applicable in the calculation of rolling and pitch problems. However, the theoretical analysis method has a large calculation error, and the effect in the rolling motion calculation is not very obvious. The accuracy of the calculation results in the application of the model test method is high. However, there are many restrictions on the error control of the test process and the requirements of the equipment. In contrast, the numerical analysis method is solved by iterative iterations by discrete methods. With the rapid improvement of computer hardware performance, it has become an important research method.

The mathematical modeling or numerical analysis is often used to study the generation mechanism of problems and their solutions, which has become a frequently used method in the field of natural sciences and practical engineering applications. The mathematical modeling through the collection of sample data information has been applied in many fields. System identification is a method that can achieve the best fit to the dynamic characteristic model of the identified system by choosing among the preset model types according to the optimization goal [18]. The specific implementation process is to first select the mathematical model related to the identified system. Then, the properly selected test signals are added, and the corresponding input and output data are recorded, or the corresponding operating data are directly used for identification. Therefore, the identification of the parameters is completed, and a model that can better fit the statistical data is selected. The selected model is evaluated by the validity test method to determine whether the corresponding object that ultimately needs to be identified can represent the corresponding characteristics of the system. If the corresponding test passes, the identification of the system will be completed; otherwise, an alternative model needs to be selected and repeated until it is valid. The genetic algorithm optimizes gene configuration based on probability. It has potential parallelism, fast and random search capabilities, simple search process using evaluation functions, and can handle discrete problems; at the same time, it also has the disadvantages of slow convergence, prone to precocity, and dependence on the initial population [19]. The implementation of the genetic algorithm

is shown in Fig. 3 below. The conventional system identification method is apt to fall into the local optimal solution due to the excessive use of the least-squares method. It is a feasible solution method to replace the global convergence algorithm with an ideal initial value or directly obtain the parameter optimization solution. The genetic algorithm just meets this requirement. The idea of system identification is introduced to equationte the types of mathematical models of amphibious armored vehicle movements. Also, the test data are optimized to determine the coefficients to be identified in the mathematical model of amphibious armored vehicle movements. In the end, the complete mathematical model of amphibious armored vehicle motion is determined, and the optimization calculation is implemented by the genetic algorithm.

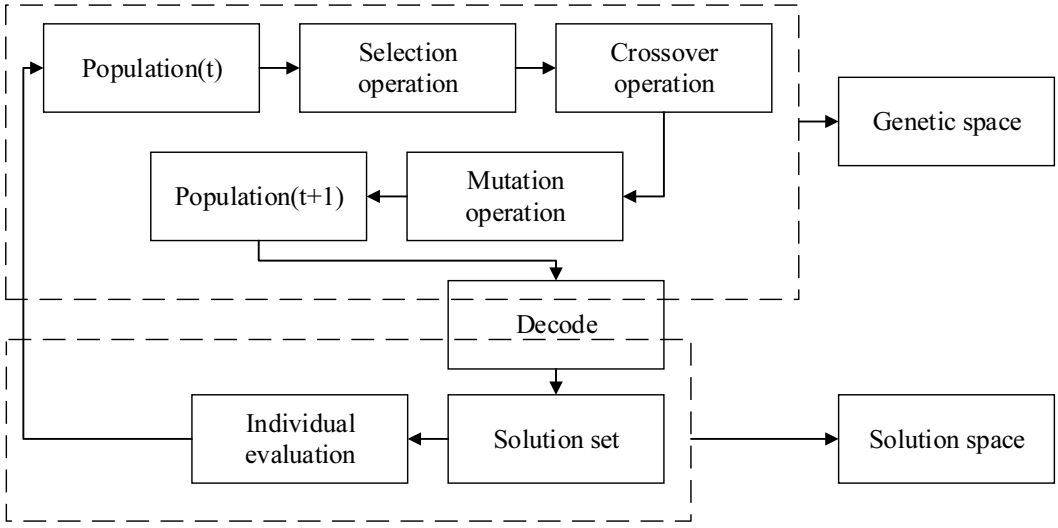

Fig. 3. Operational implementation flow of the genetic algorithm

On this basis, the model test and system identification are fused. This study brings the experimental data into the water motion model equations of amphibious armored vehicles and uses iterative methods to solve the equations to explore the rolling motion of armored vehicles. The corresponding implementation process is shown in Fig. 4 below.

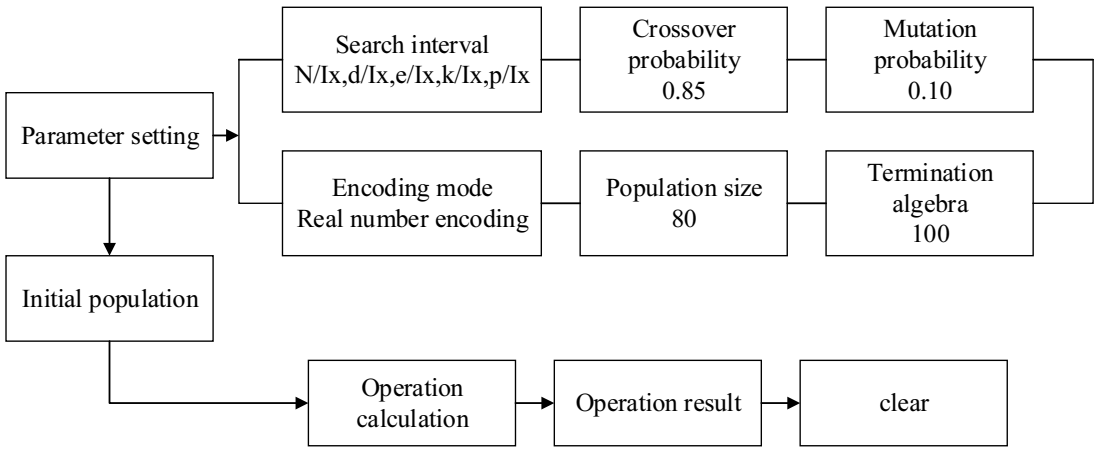

Fig. 4. The implementation process of the system identification method

3.4 Design and Model Establishment of Vehicle Rolling Test

Based on the premise that the distance between the side body and the main body of the amphibious armored vehicle is large, the recovery torque corresponding to the buoyancy generated by the side body during rolling is also large, and the moment of inertia of the vehicle body relative to the length of the vehicle is greater. Therefore, the distance between the side body and the main body is the key direction

for exploring the navigation stability of the amphibious armored vehicle. For this reason, the test for the vehicle to roll in the water is designed as follows. First, the car model is smoothly placed in the middle of the pool. To reduce the impact of the shore on the test, the vehicle length is perpendicular to the shore and the car model is floating. Then, the MTi measurement software of the computer terminal is run; the initial roll angle θ is applied, and the angle is kept between 2° and 7°. Once the car model stabilizes, the external force is applied to make the car model tilt to the left or right. While the external force is released, the data are collected by the software, the car model is allowed to roll freely, and the data will not be collected until the next time the model is stable again. The six DOF related data in the measurement software are read. By changing the distance between the front and backside bodies to the subject, the layout of the specific scheme is designed, as shown in Table 1 below.

Table 1. Scheme layout of each side body

Layout plan of the vehicle side body	a	b	c	d	e	f
Distance between the front body and the main body of the vehicle (m)	1.5	0.9	0.4	0.9	0.4	0.4
Distance between rear body and the main body of the vehicle (m)	1.5	1.5	1.5	0.9	0.9	0.4

The free decay linear differential equation of conventional armored vehicles that produces rolling motion in the water is shown in Equation (9) below. Since the distance between the side body and the main body of the vehicle is relatively large during rolling, the generated torque is large. Linear damping alone cannot accurately represent the force on the vehicle. Therefore, a nonlinear damping term is introduced into it, and the corresponding rolling mathematical model is shown in Equation (10) below.

$$I_x \ddot{\theta} + 2N_x \bar{\theta} + k_x \theta = 0 \tag{9}$$

Where: $I_x \ddot{\theta}$ is the moment of inertia, I_x is the total moment of inertia, $2N_x \bar{\theta}$ is the linear damping moment term, N_x is the corresponding damping moment coefficient, and $k_x \theta$ is the restoration moment term.

$$\dot{\theta}_{j+1} = \left(1 - \frac{2N_x \Delta t}{I_x}\right)\dot{\theta}_j - \frac{\Delta td}{I_x}\left|\dot{\theta}_j\right|\dot{\theta}_j - \frac{\Delta te}{I_x}\dot{\theta}_j^3 - \frac{\Delta tk_x}{I_x}\theta_j - \frac{\Delta tp}{I_x}\theta_j\left|\theta_j\right| \tag{10}$$

Where: $\dot{\theta}_{j+1}$ is the actual measured value at time $j+1$, θ is the rolling angle, and d, e, and p are undetermined coefficients.

The identification in this study belongs to the identification of multiple parameters. The output of the rolling motion is taken as the pre-identified design variable. The following Equation (11) is used, and the corresponding upper and lower limits are used as the constraint conditions. For the reliability test of the method proposed in this study, this study completes the test by comparing the calculated value based on the linear mathematical model and the error between the predicted value and the experimental value based on the non-linear mathematical model. The corresponding error value between the experimental values is at a relatively small level, which indicates that the method proposed in this study and the corresponding mathematical model constructed are reliable and applicable. An equation expression based on the second-order system equation that has a function of predicting the value at the next moment is shown in Equation (12) below. One of the test data obtained is subjected to the corresponding identification analysis based on the identification method of the rolling motion. By substituting the result into the above equation, the obtained curve is compared with the curve calculated by the equation and the test curve; therefore, the reliability of the constructed mathematical model can be verified.

$$X^T = \left\{N/I_x, d/I_x, e/I_x, k/I_x, p/I_x\right\} \tag{11}$$

Where: X^T represents the output, and the other terms in the equation represent the corresponding output terms.

$$\dot{\theta}_{j+1} = \left(1 - \frac{c\Delta t}{m}\right)\dot{\theta}_j - \frac{k\Delta t}{m}\theta_j \tag{12}$$

Where: c represents the damping moment, m represents the moment of inertia, and k represents the restoration moment.

4 Results

4.1 Analysis of the Hydrodynamic Model of the Amphibious Armored Vehicle

Based on the dynamic equation model of the amphibious armored vehicle constructed above, the changes in the acceleration, velocity, and position on the inertial coordinate axis of the vehicle body coordinate axis in MATLAB software are shown in Fig. 5(a), Fig. 5(b), and Fig. 5(c).

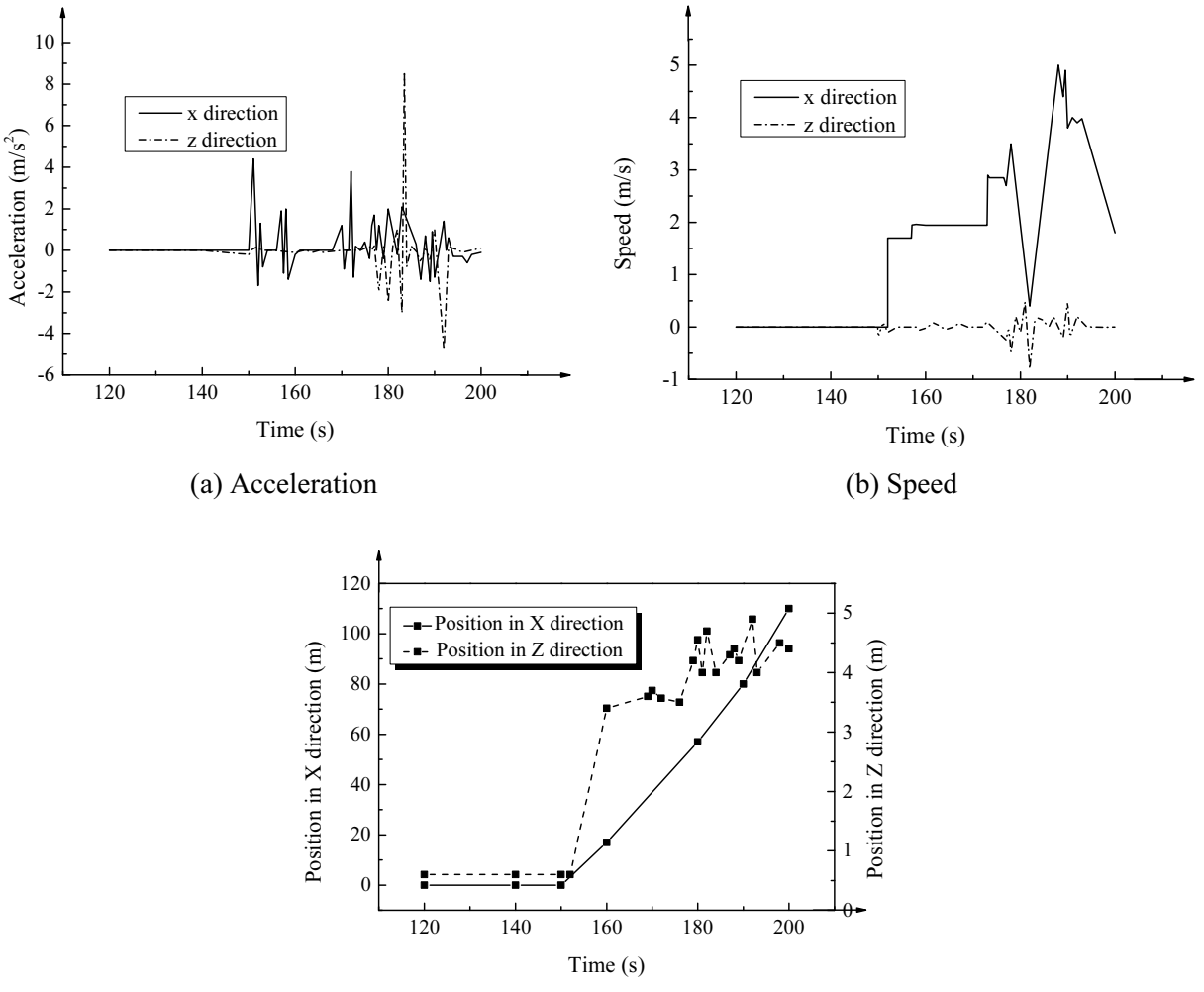

(a) Acceleration

(b) Speed

(c) Position

Fig. 5. Analysis of vehicle hydrodynamic model

As shown in Fig. 5, during the process of the amphibious armored vehicle driving from the ramp to the water, the changes in acceleration, speed, and position are relatively smooth at first. When driving to the ramp and entering the water from the ramp, due to the changes in the buoyancy, traction, and ground support forces of the vehicle, the corresponding acceleration, speed, and position of armored vehicles increase. When the armored vehicle stabilizes in the water, the changes in each parameter are stable. This elaborates that the results of the simulation analysis are better.

4.2 Reliability Verification of System Identification Method

A comparative analysis of the relative error rate between the calculated value of the linear equation and the prediction value obtained from the identification method and the experimental measurement value is performed, as well as the analysis of some errors of the identification results. The details are shown in Fig. 6 below.

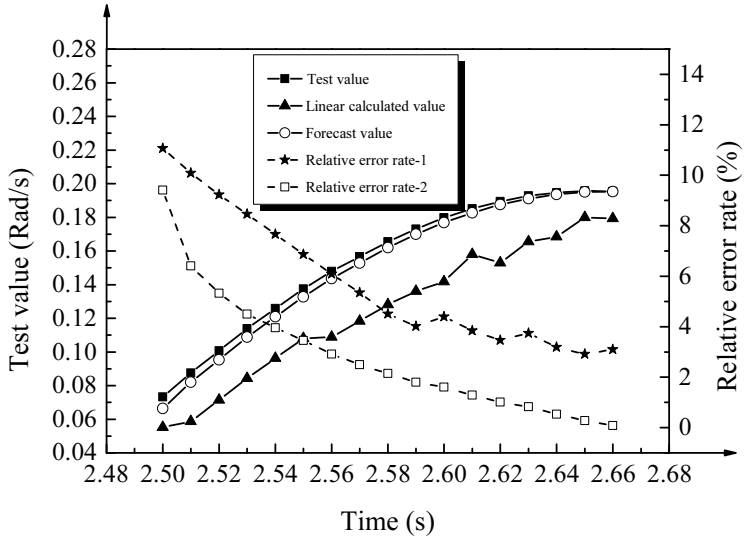

Fig. 6. Reliability verification of system identification method

As shown in Fig. 6, Relative error rate-1 is the relative error rate calculated linearly, and Relative error rate-2 is the relative error rate of the predicted value.The identification value curve obtained by the identification method in this study is closer to the experimental measurement value. The relative error rate of the prediction value curve obtained by the identification method in this study is smaller than the calculated value obtained by the linear equation. This shows that the identification method used in this study is reliable, and the corresponding mathematical equation is selected correctly.

4.3 Analysis of Vehicle Rolling Results

In the scheme a for the side body arrangement, the change curve of the initial rolling angle with time is shown in Fig. 7 below.

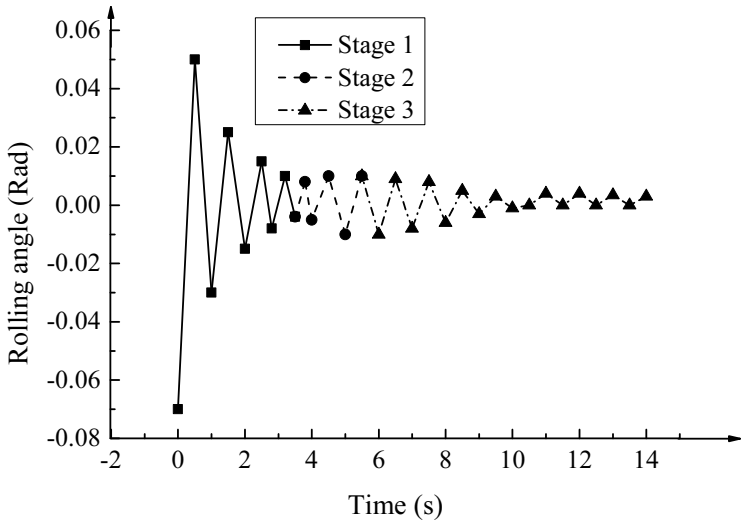

Fig. 7. Changes of vehicle initial rolling angle with time

As shown in Fig. 7, the rolling process of the amphibious armored vehicle has gone through three stages. The first stage is from the beginning to 3.32 s. The rolling amplitude of this stage shows a rapid attenuation change. From 3.32 s to 5.25 s, the rolling amplitude at this stage has an inverse increase. After the third stage corresponds to 5.25 s, the rolling amplitude at this stage gradually decreases to 0. Therefore, the identification method can be applied to the identification method proposed in this study, the linear damping component is introduced, and the three stages are identified separately. The corresponding results are shown in Fig. 8 below.

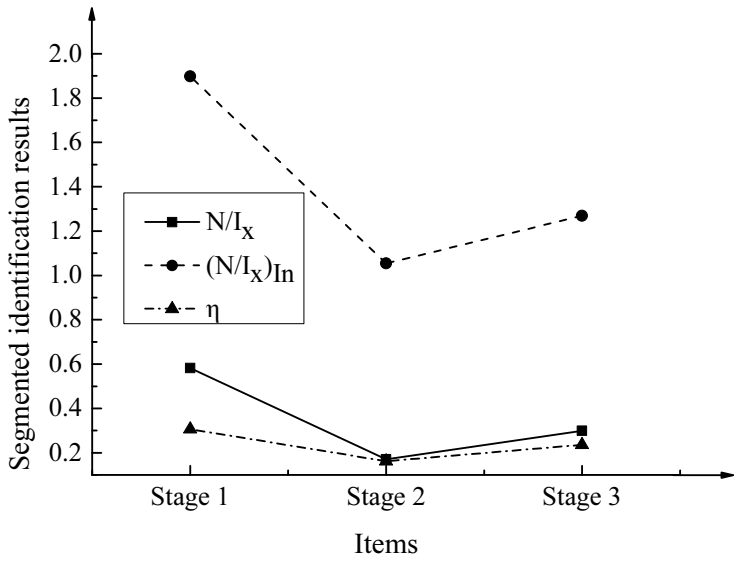

Fig. 8. Identification results of vehicle side body by scheme a

In the figure, $(N/I_x)In$ represents the calculated value of the linear equation, η is the ratio of (N/I_x) and $(N/I_x)In$, which represents the linear damping. As shown in Fig. 8, the value of η in the first stage is the largest, and the value of η in the second stage is the smallest. In the third stage, the value of η is between the two mentioned above. Thus, the interaction between the water wave caused by the main body of the armored vehicle and the body due to the rolling is an important reason for the non-linear damping in the rolling motion.

The identification results of schemes b to f for the side body layout of the amphibious armored vehicle are shown in Fig. 9 below.

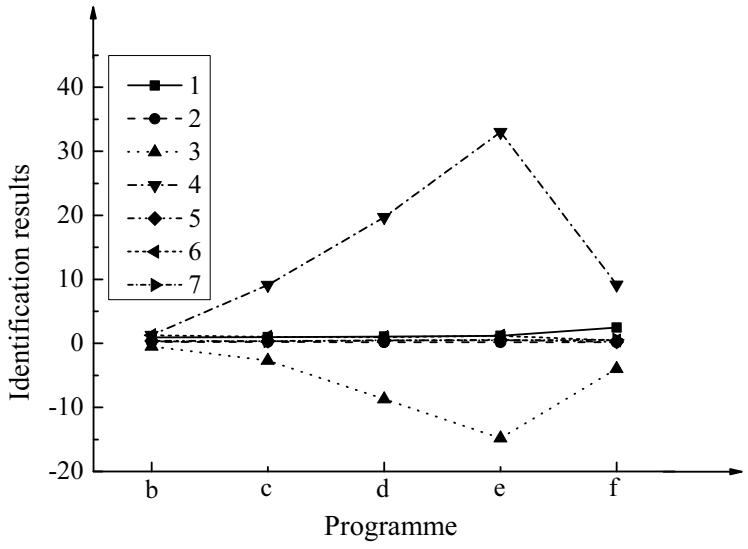

Fig. 9. Identification results of schemes b to f

In the figure, 1 is k/I_x, 2 is d/I_x, 3 is e/I_x, 4 is p/I_x, 5 is N/I_x, 6 is $(N/I_x)_{ln}$, and 7 is η.Changes in the data of the figure are analyzed. Combining the rolling amplitude changes in the side body layout scheme a, it is found that except for the obvious increase in the rolling amplitude in both schemes a and plan b, this change in other schemes is all smaller. At the same time, compared with scheme c, scheme b has a shorter period and exhibits lower attenuation and damping ratio. This may be related to the difference in the distance between the side body and the main body of the vehicle.

5 Discussion

The surface wave resistance and attitude stability are the two main aspects of the research on the navigation stability of the water surface. The study of the wave resistance is closely related to the rolling motion [20], and the rolling motion of the amphibious armored vehicle on the water is explored. Considering the effect of water on amphibious armored vehicles, it is necessary to establish the water motion model of the vehicle. Especially, the motion model that the vehicle enters the water from land has a higher reference value. Besides, the water motion model is closely related to the driving simulator. Therefore, this study combines the establishment of a driving simulator and a water sports model and the analysis of the rolling motion of an amphibious armored vehicle, hoping to expand the research direction of navigation stability of amphibious armored vehicles in the water. Vehicles passing by rivers, lakes, beaches, and other shores are mostly in the form of ramps; thus, ramp-in water is the most common situation. In this study, the simulating analysis of the amphibious armored vehicle entering the water from the land via the slope is carried out through the construction of a water movement model, and the analysis results are consistent with the actual situation.

The system identification method based on the genetic algorithm can solve nonlinear mathematical models that cannot obtain analytic solutions through optimization comparison. The difference between linear mathematical models and nonlinear mathematical models lies in the presence of higher-order terms. Therefore, in comparison, nonlinear mathematical models have higher accuracy [21]. This study uses a genetic algorithm-based system identification method to identify and analyze the rolling motion of amphibious armored vehicles. It is found that this method works well. Due to the presence of water out of the side body, both the restoration torque and the damping torque are abruptly changed; thus, simply using the linear equation cannot well describe the attitude change produced by the model. Except for the obvious errors in individual peaks and troughs, the identification method in this study has a high degree of agreement with the measured data.

This study indicates that the method can realize the segmented identification of the rolling motion of the amphibious armored vehicle in the water, which can describe the existence of the wave phenomenon to a certain extent, thereby providing a direction to study the navigation stability of the vehicle. The reverse increase of the rolling amplitude in the second stage can be considered as the result of the overlapping of the forced vibration and the free attenuation motion. Due to the different directions of resistance in the aforementioned state of motion, the superimposed damping is smaller in the case of free attenuation. In side body schemes a and b, the significant inverse increase in rolling amplitude is caused by the corresponding short roll period and the rolling amplitude attenuation in the two schemes. When the amplitude is rapidly attenuated and approaches 0, the effect of the waves between the vehicle body and the side body on the vehicle body leads to the inverse increase of the rolling amplitude. In contrast, due to the reduction of the distance between the side body and the main body, the other side body layout schemes lead to a larger period corresponding to the rolling motion and a correspondingly slower attenuation of the rolling amplitude. The car body still has a relatively high degree of rolling amplitude when it is in the car body; thus, the reverse increase in the amplitude is not very significant. In addition, compared with other schemes, in the schemes a and b, the period under the same rolling angle is shorter and the angular velocity is larger. The larger distance promotes the linear velocity. Therefore, the amplitude of the wave is larger than that of other schemes. This is also a factor that causes the reverse increase in amplitude.

6 Conclusion

In this study, a computer VR-based driving simulator is used to explore the construction of an amphibious armored vehicle hydrodynamic model and the rolling motion based on the stability of navigation wave resistance on the water. To accurately describe the situation, the system identification method based on the genetic algorithm can identify the rolling motion of the amphibious armored vehicle in sections, which provides a direction for the research of the water navigation stability of amphibious armored vehicles. However, the research in this study only considers the rolling of the amphibious vehicle on the water and the situation of entering the water from the land. The research on pitching, heaving motion, and landing of the effluent will be the direction of the subsequent study.

References

[1] B.D. Lawson, S.J. Kass, K.K. Dhillon, L.D. Milsm, T.H. Cho, A.H. Rupert, Military occupations most affected by head/sensory injuries and the potential job impact of those injuries, Military Medicine 181(8)(2016) 887-894. DOI:10.7205/MILMED-D-15-00184.

[2] M. Li, S. Guo, J. Guo, H. Hirata, H. Ishihara, Development of a biomimetic underwater microrobot for a father–son robot system, Microsystem Technologies 23(4)(2017) 849-861. DOI:10.1007/s00542-016-2817-3.

[3] F. Bolster, K. Linnau, S. Mitchell, E. Roberge, Q. Nguyen, J. Robinson., B. Lehnert, J. Gross, Emergency radiology and mass casualty incidents—report of a mass casualty incident at a level 1 trauma center, Emergency Radiology 24(1)(2016) 1-7. DOI:10.1007/s10140-016-1441-y.

[4] F.A. Cheein, Intelligent sampling technique for path tracking controllers, IEEE Transactions on Control Systems Technology 24(2)(2016) 747-755.

[5] M. Palpacelli, G. Palmieri, L. Carbonari, D. Corinaldi, Sensitivity analysis and model validation of a 2-DoF mini spherical robot, Journal of Intelligent & Robotic Systems 91(6)(2017) 1-9.

[6] M. Gianni, F. Ferri, M. Menna, F. Pirri, Adaptive robust three-dimensional trajectory tracking for actively articulated tracked vehicles, Journal of Field Robotics 33(7)(2016) 901-930.

[7] X. Zhang, B. Hou, Y. Mei, Deadbeat predictive current control of permanent magnet synchronous motors with stator current and disturbance observer, IEEE Transactions on Power Electronics 32(5)(2016) 1-1.

[8] J. Davidson, S. Giorgi, J.V. Ringwood, Identification of wave energy device models from numerical wave tank data—Part 1: numerical wave tank identification tests, IEEE Transactions on Sustainable Energy 7(3)(2016) 1012-1019.

[9] G. Nootz, S. Matt, A. Kanaev, K.P. Judd, W. Hou, Experimental and numerical study of underwater beam propagation in a Rayleigh–Bénard turbulence tank, Applied Optics 56(22)(2017) 6065-6072.

[10] L. Li, F. Yu, D. Shi, J. Shi, Z. Tian, J. Yang, X. Wang, Q. Jiang, Application of virtual reality technology in clinical medicine, American Journal of Translational Research 9(9)(2017) 3867-3880.

[11] M. Draelos, B. Keller, C. Viehland, O.M. Carrasco-Zevallos, A. Kuo, J. Izatt, Real-time visualization and interaction with static and live optical coherence tomography volumes in immersive virtual reality, Biomedical Optics Express 9(6)(2018) 2825.

[12] A. Shahar, R. Brémond, C. Villa, Can LED-based road studs improve vehicle control in curves at night? a driving simulator study, Lighting Research & Technology 50(2)(2018) 266-281.

[13] C. Purucker, F. Naujoks, A. Prill, A. Neukum, Evaluating distraction of in-vehicle information systems while driving by predicting total eyes-off-road times with keystroke level modeling, Applied Ergonomics 58(1)(2017) 543-554.

[14] H. Zhu, J. Yang, Y. Zhang, X. Feng, Z. Ma, Nonlinear dynamic model of air spring with a damper for vehicle ride comfort, Nonlinear Dynamics 89(2)(2017) 1545-1568.

[15] S.F. Abtahi, M.M. Alishahi, E.A. Yazdi, Identification of pitch dynamics of an autonomous underwater vehicle using sensor fusion, China Ocean Engineering 33(5)(2019) 563-572.

[16] Y. Lin, N. Ma, X. Gu, Springing response rapid analysis of the very large container ship, Chuan Bo Li Xue/Journal of Ship Mechanics 23(5)(2019) 575-582.

[17] R. Menayo, A. Manzanares, F. Segado, Complexity, regularity and non-linear behavior in human eye movements: analyzing the dynamics of gaze in virtual sailing programs, Symmetry 10(10)(2018) 528.

[18] V. Acharya, P. Kumar, Identification and red blood cell automated counting from blood smear images using computer-aided system, Medical & Biological Engineering & Computing 56(3)(2018) 483-489.

[19] C.M. Chan, H.L. Bai, D.Q. He, Blade shape optimization of the Savonius wind turbine using a genetic algorithm, Applied Energy 213(2018) 148-157.

[20] L. Chen, Design and experiment of hybrid stabilized tracking platform and its control system, Transactions of the Chinese Society of Agricultural Engineering 34(1)(2018) 22-27.

[21] P. Henning, D. Peterseim, Crank-Nicolson Galerkin approximations to nonlinear Schrödinger equations with rough potentials, Mathematical Models & Methods in Applied Sciences 27(11)(2017) 2147-2184.